Picosecond photoelectron spectroscopy of excited states at Si(111)$\sqrt{3}\times\sqrt{3}R$ 30°-B, Si(111)7×7, Si(100)2×1, and laser-annealed Si(111)1×1 surfaces

Mark W. Rowe, Hanli Liu, G. P. Williams, Jr., and R. T. Williams
Department of Physics, Wake Forest University, Winston-Salem, North Carolina 27109
(Received 19 May 1992; revised manuscript received 9 September 1992)

Photoelectron spectra resulting from sequential or simultaneous absorption of two photons have been studied at four different silicon surfaces. To study energy-relaxation lifetimes, one laser pulse populates conduction states and normally unoccupied surface states, from which photoelectrons are excited by the second pulse after a preset delay. Laser pulses of 1–3-ps duration in the energy range 2.33–4.66 eV are employed at repetition rates up to 82 MHz. Very high two-photon photoelectron-count rates are achieved with the methods described, while the sample temperature remains far below thresholds for melting, and space-charge effects are negligible. Surface states, particularly within the bulk band gap, are very prominent in these experiments. Hot-electron intermediate states above the conduction-band minimum (CBM) are observed, and two spectral features that persist on different surfaces are attributed to peaks in the density of conduction states of the bulk-band structure, specifically along Λ and at Γ. The near-surface population of electrons at the CBM is strongly limited by capture in surface states and by diffusion into the bulk. Photoelectron emission from the CBM excited by 4.0–4.66-eV photons is observed only by indirect transitions or scattering via surface states and defects.

I. INTRODUCTION

Nonequilibrium states in semiconductors have been studied using a variety of optical and electronic methods probing hot-carrier relaxation, high-density electron-hole plasmas, laser annealing and damage phenomena, and surface recombination, for example.[1] Equilibration of the excited carriers can be studied with explicit time resolution by excitation-probe techniques. In the work we shall describe, photoelectron emission from transiently populated intermediate states is measured.

Techniques of two-photon or two-step photoelectron spectroscopy have been developed and refined in various laboratories since about 1980. One purpose of this paper is to describe the first application of high-repetition (82 MHz), modest fluence, high peak-power picosecond pulses to excited-state photoemission spectroscopy in semiconductors, yielding two-photon signal rates up to 10^5 counts per second. We have made a comparative study of four surfaces of silicon, including the first picosecond time-resolved data reported for these surfaces, and the first two-photon photoemission results of any kind on Si(111)$\sqrt{3}\times\sqrt{3}R$ 30°-B. To place our measurements in context, we will briefly review previous work on silicon using two-photon photoemission.

The first photoemission spectra of laser excited Si(111) were measured by synchrotron radiation,[2] counting in a 1-μs gate period coinciding with 150-ns pulses of 2.33-eV laser light at 600 Hz and 60 mJ/cm^2/pulse. No photoemission from transiently populated conduction-band states or surface states was seen, but surprisingly strong modifications of the Si 2p core-level spectrum and the valence spectrum upon laser excitation were reported. Although mechanisms exist for some degree of carrier confinement,[3] later observations of Si 2p core photoemission under combined 20-ns laser pulses and synchrotron radiation[4] have not confirmed the existence of strong 2p core-hole screening on this time scale by the laser-induced plasma.

Bensoussan *et al.*[5] demonstrated two-photon photoemission from Si(111)7×7, finding a quadratic dependence of total electron yield on laser intensity and a photon-energy threshold for this process at half the work function ($\phi/2=2.3$ eV). Electron-energy spectra of the 7×7 surface were measured under excitation by 5-ns laser pulses at ≤ 100 Hz tunable from 2.3 to 4.4 eV.[6,7] They observed a spectrum of width $2h\nu-\phi$, including a peak suggested to arise from a maximum in the density of intermediate states about 2.8 eV above the valence-band edge. No feature specifically identifiable with the conduction-band minimum was found.

Long *et al.*[8] measured electron-energy spectra of Si(111)7×7 under excitation by 60-ns pulses of 4.66- and 2.33-eV light at a 1-kHz repetition rate, using a cylindrical mirror analyzer. A feature in the two-photon photoemission spectrum corresponding to emission from intermediate states 0.5 eV above the Fermi level (E_F) was resolved for the first time and was attributed to a transient electron population at the conduction-band minimum (CBM). By fitting the surface-state peak and the CBM shoulder to the Fowler-Dubridge theory of thermally assisted photoemission,[9] surface and bulk electron temperatures were deduced.[8,10] Two-pulse experiments of a different kind, using synchrotron radiation to probe band-bending dynamics via shifts of the photoelectron spectrum at variable delays after pulses from a copper vapor laser, allowed detailed surface recombination kinetics on Si(111)7×7 to be explored in the 10-ns to 10-μs time range.[4]

Bokor and co-workers raised the probe laser photon energy and reduced the pulse duration in angle-resolved studies of the cleaved Si(111)2×1 surface.[11] The 10.5-eV

probe photons were generated in xenon as the ninth harmonic of a 60-ps Nd:YAG laser pulse (where YAG denotes yttrium aluminum garnet). Amplification required for uv harmonic generation limited the repetition rate to 10 Hz, but signal rate was regained by the use of time-of-flight electron analysis to acquire data in parallel energy channels. With 60-ps pulses, they were able to conduct delayed-probe time-resolved photoelectron measurements on silicon for the first time.

Using a 0.44-eV pump pulse derived from the Nd:YAG fundamental by stimulated Raman scattering in methane, electrons were excited directly from the π surface states to the vacant π^* surface states on Si(111)2×1. The population recovery was observed by photoemission as a function of probe delay.[11] Because the 10.5-eV probe photon energy substantially exceeded the sample's work function, they could excite photoelectrons from states well below E_F, observing depopulation of the π surface state and photovoltage shifts of valence-band features. Partly offsetting these advantages of a vacuum ultraviolet probe, space-charge effects of the large current associated with one-photon valence-band photoemission limit the probe fluence that may be usefully employed and, hence, the two-photon signal rate.[12]

Using 2.34-eV excitation photons and probe energies of 10.5 and 4.68 eV, Halas and Bokor[13] measured the time-dependent population of the π^* surface state and the bulk (near-surface) conduction-band minimum, respectively, on Si(111)2×1. The lifetime of the π^* population against recombination mediated by surface defect sites was $\tau \approx 200$ ps on the clean 2×1 surface. The data implied large surface recombination velocities in the low-injection regime: $\sim 3\times 10^7$ cm/s on n-type and $\sim 3\times 10^4$ cm/s on p-type samples of Si(111)2×1.

Aside from the work on silicon discussed above, the method of two-photon photoelectron spectroscopy has been applied to a number of other semiconductor[14–19] and metal[20–23] samples.

One goal of the work reported here was to develop and explore an alternative experimental approach utilizing a much higher repetition rate of the laser source and lower energy per pulse than in the experiments reviewed above. Different aspects of the laser-excited solid are probed as functions of energy density and of pulse duration. Some of the prior work on two-photon photoemission has been directed toward laser-induced melting or structural changes.[5–8,10] This investigation, as an application of picosecond two-photon photoelectron spectroscopy at MHz repetition rates, may be described as "gentle probing" of the sample in terms of energy fluence, although the peak intensity is certainly within the nonlinear regime.

Our experiments provide new data on the excited-state properties of four different silicon surfaces. This is the first reported study of the Si(111)$\sqrt{3}\times\sqrt{3}R$ 30°-B surface by two-photon photoelectron spectroscopy. In general, a $\sqrt{3}\times\sqrt{3}$ reconstruction of the (111) surface of silicon is induced by adsorption of column-III metals, including Al, Ga, and In, on the surface such that they occupy the adatom (T_4) site in the surface unit cell.[24] Boron, in contrast, is incorporated in *subsurface* fivefold-coordinated sites (S_5) directly below Si adatoms in T_4 sites.[25–27] A $\frac{1}{3}$-monolayer coverage in such subsurface sites drives the $\sqrt{3}\times\sqrt{3}$ reconstruction in the surface layer, which remains pure silicon in principle. The ideal reconstructed surface has no occupied states in the gap and is comparatively passive. The Si-B back-bond state can be seen in ultraviolet photoemission at a binding energy of ~ 1 eV with respect to the valence-band maximum.[28] The properties of this surface have been intensively studied since the discovery in 1989 of the subsurface boron site and its unusual role in the reconstruction.[25–30]

We also present picosecond time-resolved photoelectron spectroscopy on the 7×7 silicon surface. The surface states have a metallic distribution within the gap on Si(111)7×7.[31–34] Prior measurements have indicated large surface recombination velocities of order 10^6 cm/s on the 7×7 surface of both n- and p-type Si.[4] The observation of a CBM feature in two-photon photoelectron spectra measured with 4.66-eV light on (111) surfaces in this work and earlier experiments[7,11] may seem puzzling because a direct 4.66-eV transition from the conduction-band minimum (near X) provides insufficient momentum normal to the (111) surface for escape. It is therefore interesting to compare a (100) surface. Specifically, the Si(100)2×1 surface has been studied. Laser-annealed silicon (111) 1×1 has been included among the surfaces studied.

Whereas the surface-state contributions to the two-photon photoemission measurements are expected to vary widely among the four surfaces studied, the comparisons of different surfaces were also undertaken to look for aspects that remain the same. We have attempted to identify features in the hot-electron spectrum with the bulk-band structure of silicon, and have encountered bulk diffusion as an important factor determining population dynamics in the near-surface region.

II. EXPERIMENT

Photoelectron spectroscopy was conducted in ultrahigh vacuum (UHV) at a working pressure of 4×10^{-10} torr (5.3×10^{-8} Pa). Electron-energy analysis and Auger spectroscopy were accomplished with a double-pass cylindrical mirror analyzer (CMA). A plano-convex silica lens with 50-mm focal length was positioned inside the vacuum chamber to focus the laser light on the sample at the electron focus of the CMA. The lens produced a Gaussian beam waist diameter of approximately 10 μm for 4.66-eV light. Minimum spot size on the sample was achieved by translating the lens along the optical axis to maximize photoelectron counts in the two-photon part of the spectrum characterized by quadratic dependence on laser intensity. The peak in count rate at minimum spot size was quite sharp and served as a reliable criterion of best focus.

The sample was biased negative (≈ -9.5 V as noted for specific data) to improve CMA transmission efficiency. The bias voltage appears as a simple offset of the photoelectron spectra, and accounts for the fact that spectra presented as raw data include electron energies up to 14 eV. Electrons were detected by a channeltron in

pulse-counting mode.

Low-energy electron diffraction (LEED) was used to characterize the surface structure of each sample following preparation by sputter etching and/or annealing. Sample introduction and preparation were carried out in a UHV side chamber so that the photoelectron spectroscopy chamber rarely came up to air. Auger analysis was performed at the conclusion of each experiment.

The laser system was based on an actively mode-locked Nd:YAG oscillator emitting a continuous train of pulses at an 82-MHz repetition rate. After passing through a fiber-grating pulse compressor, the 1.06-μm pulses were frequency doubled in potassium titanyl phosphate and redoubled in a 3-mm potassium dihydrogen phosphate crystal providing 3-ps pulses of 2.33- and 4.66-eV light. (The 0.9-ps contribution of group velocity dispersion in the second doubling crystal to uv pulse broadening is approximately offset by the shortening effect of squaring the Gaussian pulse shape.) Because 4.66 eV is a particularly useful photon energy relative to the work function of silicon, these pulses were employed for much of the work to be reported, despite the availability of shorter pulses from the dye laser at lower photon energies.

For shorter pulses and wavelength tunability, a dye laser was synchronously pumped by the 3-ps, 532-nm pulses. This yielded 500–800-fs pulses at 82 MHz, measured by a scanning autocorrelator. The dye tuning range yielded frequency-doubled photon energies from 3.92 to 4.19 eV. For some experiments, the repetition rate was lowered to 4 MHz or less and the pulse energy was raised by use of a cavity dumper in the dye laser.[35]

For even shorter pulses, which we consider important for pushing the resolution of this method to the interaction time scale of an optical phonon period, a second (fiber-prism) pulse compressor was added after the synchronously mode-locked dye laser. This yields an 82-MHz train of pulses having widths of 90 fs, measured by autocorrelation of the dye fundamental. Preliminary time-resolved measurements have been made using these pulses, although the present 3-mm doubling crystal broadened the 4.22-eV probe width to about 700 fs. Further results with a shorter uv probe will be presented in future work.

Time resolution of the intermediate-state population was obtained by splitting the pulse train into two parts and delaying one part relative to the other. The experiments can be characterized as "one color" or "two color" in the following sense. If both the excitation and probe pulses have the same photon energy, i.e., derived by splitting a single ultraviolet pulse train, the photoelectron yield versus pulse delay is a symmetric convolution of the identical pump and probe pulses with the lifetime of electrons in the intermediate state. Alternatively, the 2.33- and 4.66-eV pulses could be separated to form synchronized excitation and probe pulses at different wavelengths. It is crucial that the delayed and recombined beams be colinear and overlapping upon entry to the experiment chamber in order to assure overlap of the respective spots on the sample. We achieved this by mutual centering of the beams over a six-meter distance between the delay line and the chamber. The energy of the intermediate state probed is the final photoelectron energy selected by the CMA minus the probe photon energy, taking appropriate account of the detector work function and sample bias as described below. Thus, this experiment allows selection of specific intermediate states whose populations can be followed as a function of time delay.

It is useful to consider the magnitudes of several of the parameters of this experiment. A variety of pulse durations, peak intensities, repetition rates, and photon energies were used in obtaining the results reported below. Three of the most important cases are summarized in Table I, which also lists energy fluence per pulse, average power, absorption coefficients, maximum count rate, and electrons emitted per pulse. When 4.66 eV was used as the probe photon energy, the uv spot was defocused somewhat to compromise with the green pump focus, since the lens was not a uv achromat.

Note that the excitation pulse energy in this experiment is in the range 0.07–1.8 nJ, compared to typical mJ pulse energies used in the prior experiments reviewed above. Because of the small spot size and short pulse duration employed in this work, a 70-pJ pulse translates to a peak intensity on sample of up to 30 MW/cm^2 for 3-ps, 4.66-eV pulses. At such intensities, two-photon excitations are readily observed and very short-lived inter-

TABLE I. Representative parameters of this experiment.

Photon energy	(eV)	4.66	2.33	4.0
Pulse duration	(ps)	3	3	1.2
Repetition rate	(MHz)	82	82	4
Average power	(mW)	6	150	2
Pulse energy	(nJ)	0.073	1.83	0.5
Spot diameter	(μm)	10	~50	10
Energy fluence	(μJ/cm^2)	93	93	700
Peak intensity	(MW/cm^2)	31	31	584
Max counts/s	(s^{-1})	10^6		10^4
Counts/pulse		0.012		0.002
Electrons/pulse		~60		~10
Average T	(°C)	22	30	22
ΔT/pulse	(°C)	6	<1	<85
Si absorption coefficient	(cm^{-1})	2.1×10^6	1.2×10^4	1.45×10^6
Excitation density	(cm^{-3})	10^{20}	3×10^{18}	10^{21}

mediate states may be probed. The maximum electron count per pulse per 0.18-eV CMA bandpass is only about 0.012 electron, but this yields 10^6 counts per second at an 82-MHz repetition rate. The total electron emission per pulse integrated over energy and angle, whether counted by the detector or not, is about 50. This is well below the onset of space-charge effects, which set an upper limit on the count rates that could be usefully acquired in Refs. 5, 6, 11, 12, and 15 at high intensity.

The typical 6-mW ultraviolet-beam power in this experiment produces a negligible average temperature rise of the sample. Using one-dimensional heat-flow simulations[35] and verifying with analytic approximations,[36] we find that our typical 93-μJ/cm^2 peak fluence at 4.66 eV produces a peak lattice temperature rise of only 6 °C. The temperature recovers to the average sample temperature (approximately equal to room temperature) before the arrival of the next pulse 12 ns later. For the 2.33-eV pump pulse, the peak temperature rise is less than 1 °C because the Si absorption coefficient is lower. Under illumination by the 150-mW beam of 2.33-eV light used in two-color time-dependence studies, the average temperature rises only about 10 °C in a run. It is clear that this experiment is conducted far below thresholds for annealing or surface phase transitions on silicon. This situation is to be contrasted to Refs. 5–8, 10, and 37, where a specific intent of the experiments was to explore energy deposition and relaxation for fluences extending through the annealing threshold. The method we describe here is well suited to study electronic excited states with very little lattice heating and no irreversible changes in the crystal.

III. RESULTS

The experimental results for each of the four surfaces studied are presented below.

A. Si(111)$\sqrt{3}\times\sqrt{3}R$ 30°-B

Samples were prepared by implanting silicon (111) wafers with 30-keV boron ions at 2×10^{16} cm^{-2}, resulting in a boron concentration of $\sim1.5\times10^{20}$ cm^{-3} near the surface. The implanted wafers were annealed for 90 min at 1050 °C, chemically cleaned, and protected with a thin oxide layer. The oxide cap was etched in hydrofluoric acid prior to introducing the sample into UHV. The samples were sputter etched in UHV with an argon ion gun and then annealed for two cycles of 5 min at 1000 °C. Boron diffuses to the surface during annealing, where it incorporates as $\frac{1}{3}$ monolayer occupying the S_5 substitutional sites in uppermost silicon bilayer beneath silicon adatom sites.[38] Boron occupancy of these subsurface sites drives the $\sqrt{3}\times\sqrt{3}$ reconstruction, which we verified for each sample by LEED observations. Ultraviolet photoemission shows that the surface is metallic in that E_F lies within the boron-modified valence band.[38] Auger analysis performed at the conclusion of each photoelectron experiment showed that the surfaces remained clean, with typical peak ratios of O(KLL)/Si(LMM) <0.005 and C(KLL)/Si(LMM) <0.03.

Photoelectron spectra for Si(111)$\sqrt{3}\times\sqrt{3}R$ 30°-B under excitation by 3-ps pulses of 4.66-eV light are given in Fig. 1 for peak laser intensities ranging from 0.52 to 26.9 MW/cm.[2] The sample bias was -9.77 V. Taking into account the CMA work function (4.52 eV), the kinetic energy of a photoelectron excited from the Fermi level by one 4.66-eV probe photon corresponds to 9.91 eV in Fig. 1 (energy scale at top). Thus the initial states accounting for the strong peak near 9.9 eV lie at and slightly below the Fermi level, consistent with the observed linear dependence of this peak on laser intensity. The bulk Fermi level in these heavily doped samples is degenerate with the top of the valence band. The vacuum energy is estimated to be 9.8 eV, judging from the onset of the spectrum in Fig. 1, so that we obtain the work function $\phi\approx4.55$ eV for this surface.

There is no shift of the linear photoemission peak energy with laser intensity in Fig. 1, indicating that band bending is zero on this surface, or that the photovoltage shift already saturated at a lower intensity. The absence of photovoltage shifts on the $\sqrt{3}\times\sqrt{3}$ surface is consistent with the expectation of flat bands in equilibrium on the ideal Si(111)$\sqrt{3}\times\sqrt{3}R$ 30°-B surface, due to the absence of occupied surface states in the gap.[25] McLean, Terminello, and Himpsel observed band bending on $\sqrt{3}\times\sqrt{3}$ surfaces prepared by annealing bulk-doped Si:B

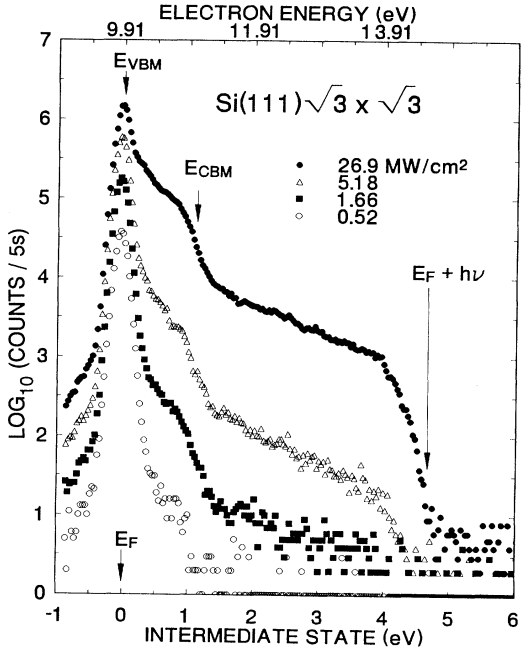

FIG. 1. Photoelectron spectra for Si(111)$\sqrt{3}\times\sqrt{3}R$ 30°-B excited by 3-ps pulses of 4.66-eV light at the peak intensities shown. The energy scale at the top is the measured electron kinetic energy, including the -9.77-V sample bias. The energy scale at the bottom is the two-photon intermediate state relative to the Fermi energy as zero, defined as E_i in Eq. (1). The logarithm of electron counts per 5-s interval is plotted.

wafers, and suggested that the Fermi level might be pinned in that case by patches of 7×7 structure in which the boron $\frac{1}{3}$ monolayer is incomplete.[25] In comparison, the absence of band bending on our samples indicates that the $\sqrt{3}\times\sqrt{3}$ surface prepared by ion implantation and annealing is single domain, in agreement with other studies using these samples.[38]

The entire photoelectron spectrum above 10 eV in Fig. 1 is quadratic in laser intensity, indicating that two photons participate in the transitions. Note that the scale of electron counts per 5-s interval is logarithmic, covering more than six decades. It is helpful to think of the final-state energies plotted in Fig. 1 as lying one probe photon (4.66 eV) higher than a corresponding intermediate state E_i. Specifically, if the intermediate state E_i is defined relative to the Fermi energy E_F, and if E_k is the final-state kinetic energy, $h\nu$ is the probe photon energy, V_b is the magnitude of the negative sample bias, and ϕ_d is the detector work function, then the photoelectron kinetic energies measured are

$$E_k = E_i + h\nu + eV_b - \phi_d \ . \tag{1}$$

Since V_b, ϕ_d, and $h\nu$ are constants in a given experiment, we can just as well plot the experimental spectra against

$$E_i = E_k - eV_b - h\nu + \phi_d \ ,$$

obtaining the photoelectron spectrum versus intermediate-state energies. This scale is used at the bottom of Fig. 1 and each succeeding electron-energy spectrum. The electron kinetic energy E_k is given at the top of each spectrum.

Relative to the E_i scale, we have marked E_F $(=0)$, $E_{\rm VBM}$, $E_{\rm CBM}$, and $E_F+h\nu$ (where VBM and CBM denote the valence-band maximum and conduction-band minimum, respectively). The latter energy $(E_F+h\nu)$ represents the highest intermediate state than can be populated by the pump photon energy, which, in this case, is the same as the probe photon. Recall that E_i was defined relative to the sample's Fermi level. If E_i is positive, then one photon is required to populate the intermediate state, either directly or indirectly. A second photon is required to complete the photoelectron excitation. It is represented as the energy $h\nu$ appearing in Eq. (1). We have measured laser-power dependence throughout the spectrum of Fig. 1. Photoemission via states with $E_i>0$ is approximately quadratic in laser intensity, while photoemission via states with $E_i\le 0$ has a linear dependence on laser intensity.

The plateau from $\sim$1.2 eV up to the two-photon limit at 4.66 eV in Fig. 1 involves intermediate states above the conduction-band minimum. Although the plateau is relatively featureless, the step at $E_i=3.9$ eV is significant when compared to corresponding spectra on other surfaces and to the silicon band structure. The latter correspondence will be discussed after results for the other surfaces have been presented.

The most remarkable feature about Fig. 1 is the prominence of two-photon photoemission from intermediate states throughout the band gap, compared to the plateau associated with hot-carrier states in the conduction band and possible surface states degenerate with it. The conduction-band minimum does not show up as a peak here, being at most a shoulder at the upper edge of the gap-state contribution. As shown in the expanded linear plot of Fig. 2, there are two significant bumps in the density of transiently occupied intermediate states within the band gap. The approximate decomposition shown in the figure, assuming symmetric peaks for simplicity, suggests that one surface-state band is about 0.2 eV above the valence-band maximum (VBM$\approx E_F$), and the other is about 0.6 eV above the VBM. Scanning tunneling spectroscopy of Si(111)$\sqrt{3}\times\sqrt{3}$-B has shown unoccupied surface states approximately 0.5 and 1.4 eV above the VBM.[26,39–41] The 1.4-eV surface-state band was associated with "dark" silicon adatoms atop the boron-substituted sites on imperfectly ordered surfaces,[26,40] and with all Si adatoms on a single-domain $\sqrt{3}\times\sqrt{3}$ surface produced by exposure of Si 7×7 to 1 L decaborane and annealing to 1000 °C.[40] On the single-domain $\sqrt{3}\times\sqrt{3}$ surface, a gap was found between the -1.8-eV occupied surface-state and the $+1.4$-eV unoccupied surface-state band. Bedrossian *et al.* observed that the lower-energy side of the 1.4-eV surface-state band extended through the upper $\frac{2}{3}$ of the bulk-band gap.[26]

Angle-resolved inverse photoemission also reveals the unoccupied surface state near 1.4 eV.[28] Its dispersion curve, measured along $\bar{K}$-$\bar{\Gamma}$-$\bar{M}$, extends from a minimum at approximately 1.3 eV above the VBM to a maximum at approximately 1.7 eV. It was attributed to an empty dangling-bond orbital on the silicon adatom above the boron, as was the corresponding feature in scanning-tunnel-microscopy (STM) spectra. The 1.4-eV peak is degenerate with the conduction band, and does not appear as a strong intermediate state in our experiment. One reason for its weakness in this experiment may be found in the discussion of carrier diffusion below. That is, electrons in surface states degenerate with the conduction band may scatter to conduction states and diffuse into the bulk.

Bedrossian *et al.*[26] and Lyo, Kaxiras, and Avouris[40] associated the 0.5-eV surface state with "bright" silicon adatoms in STM images of imperfectly reconstructed surfaces, i.e., where boron does not occupy the substitutional site below. They considered the surface states due to

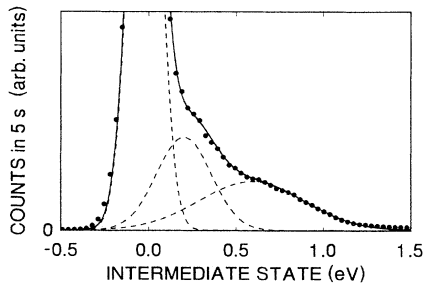

FIG. 2. Part of the photoelectron spectrum of Fig. 1, corresponding to the region of the bulk-band gap, is plotted on a linear scale of counts and decomposed into three symmetric bands with peaks at 0, 0.2, and 0.6 eV relative to the Fermi energy.

such adatoms to be comparable to the dangling-bond surface states on Si(111)7×7. On the other hand, Kochanski has seen indications of a 0.5-eV surface state in STM spectroscopy on single-domain Si:$\sqrt{3}\times\sqrt{3}$-B with the full $\frac{1}{3}$ monolayer of subsurface boron.[41] The samples for the latter study were ion implanted identically to ours and were prepared by a similar sputtering and annealing procedure in UHV. The STM images[41] showed that essentially all of the atoms were equivalent, with an upper limit on the defect fraction of 1%. Among the unoccupied surface states we observe throughout the bulk band gap, the peak we have assigned at 0.6 eV above E_F is consistent with the 0.5-eV surface state found in the preliminary STM data of Kochanski on the $\sqrt{3}\times\sqrt{3}$ boron-implanted surface.[41] The surface-state peaks observed on $\sqrt{3}\times\sqrt{3}$ Si:B by STM are of order of 1 eV in width, in rough agreement with the bands used for the spectral decomposition in Fig. 2.

The intermediate state 0.2 eV above E_F, which is quite evident in our data, does not show up in the STM density of states.[26–40] Part of the difference may have to do with the vanishing sensitivity of the STM as the probed energy approaches E_F (zero tip bias). However, some remnant of a strong surface state 0.2 eV above E_F should be seen by STM if it is present. Failure to observe it in the tunneling spectrum suggests that it is not a surface state at all. The intermediate state at approximately 0.2 eV (± 0.15 eV) in our data may be attributable to boron acceptors within the photoelectron escape range in these degenerately doped ($\approx 1.5\times 10^{20}$ cm^{-3}) samples. Neutral acceptors could acquire electrons photoexcited from the valence band and thus appear as pumped intermediates, while the negative acceptors contribute to the linear photoemission. With an average uv photon flux of $\sim 10^{16}$ photons/s, this experiment is capable of extraordinary sensitivity to minority states, including bulk dopants.

Time-resolved data for the $\sqrt{3}\times\sqrt{3}$ surface are shown in Fig. 3, where photoelectron counts are plotted against relative delay of 2.33-eV and 4.66-eV pulses. Positive delay corresponds to the 2.33-eV pulse preceding the 4.66-eV pulse. Each time-dependence curve is labeled by the intermediate state E_i defined in Eq. (1) for $h\nu=4.66$ eV. Since there is no photovoltage on this $\sqrt{3}\times\sqrt{3}$ surface, E_i is measured relative to the Fermi level in Fig. 3. In the case of positive delay, the probe photon energy is 4.66 eV and the E_i labels relate directly to the intermediate states in Fig. 1. For negative delays, the probe photon energy is $h\nu=2.33$ eV, so that the intermediate states being probed lie 2.33 eV higher than the labeled E_i values, i.e., high above the CBM. The short lifetime of electrons in these states imparts a sharp rising edge to the time-dependence trace, as observed in Fig. 3. Data were measured out to 400-ps delay, and showed no significant lifetime longer than about 70 ps.

The data have been fitted to two components of exponential decay as summarized in Fig. 4, where the lifetimes are plotted versus intermediate-state energy relative to the valence-band edge. (For the degenerate p-type doping of this sample, E_F and the VBM nearly coincide, so the energy plotted on the horizontal axis is E_i, as defined earlier. Exponential decay times have been assumed for convenience in parameterizing lifetime data, although the electron-energy relaxation is generally not an exponential function of time.[11–13]) All lifetimes in Fig. 4 refer to surface states within the bulk-band gap. The principal component of the intermediate-state lifetime decreases from a maximum of 8 ps measured 0.2 eV above the valence-band edge to 4.5 ps measured just below the conduction-band minimum. A secondary, longer-lifetime component is observed decreasing from about 60 to 20 ps over the same energy range, while simultaneously decreasing in amplitude.

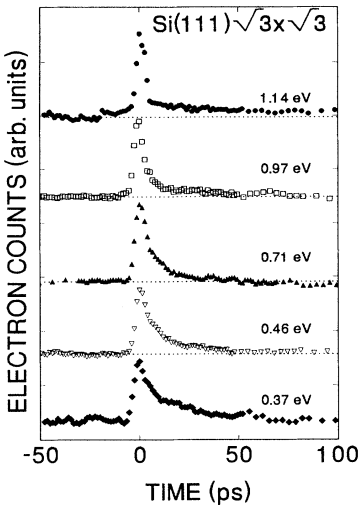

FIG. 3. Time-resolved two-photon photoemission plotted as a function of delay between the 2.33-eV excitation pulse and the 4.66-eV probe pulse. The curves are labeled by the intermediate-state energy relative to the Fermi level. The conduction-band minimum corresponds approximately to $E_i=1.14$ eV. Pulse durations were 3 ps.

Time-resolved measurements were also made in which both pump and probe pulses had the same photon energy, 4.66 eV. In this case, the plot of photoelectron counts versus delay between identical pulses should be symmetric about zero delay, and any excess width compared to optical autocorrelation arises from the persistence time of excited electrons created by one pulse and probed by the other. Curves plotted through the data in Fig. 5 are convolutions of the widths of the 3-ps excitation and

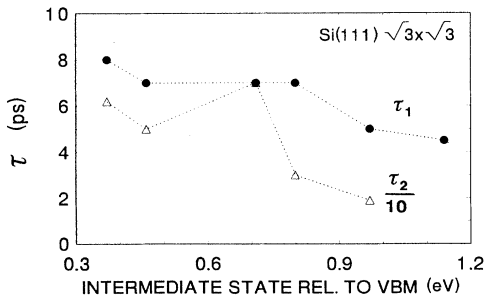

FIG. 4. The intermediate-state lifetimes obtained by fitting the data of Fig. 3 are plotted vs intermediate-state energy measured relative to the valence-band maximum (VBM). The long-lifetime component τ_2 is plotted as $\tau_2/10$.

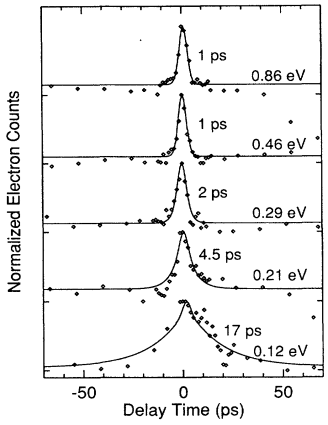

FIG. 5. Time-resolved photoemission plotted as a function of delay between two identical 3-ps pulses of 4.66-eV photons on Si$\sqrt{3}\times\sqrt{3}R30°$-B. The data are labeled by the intermediate-state energy relative to the Fermi level, defined as E_i in Eq. (1). The curves through the data are the result of convoluting the 3-ps excitation and probe pulses with a single exponential lifetime of the intermediate state, as listed in the figure.

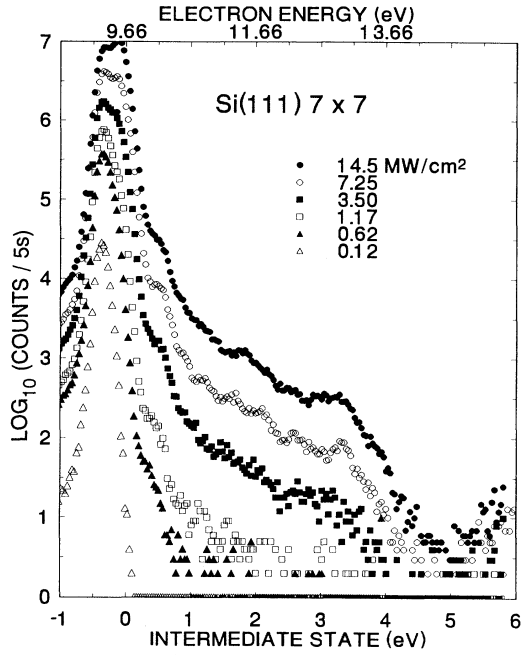

FIG. 6. Photoelectron spectra for Si(111)7×7 excited by 3-ps pulses of 4.66-eV light at the peak intensities shown. The energy scale at the top is the measured electron kinetic energy, including the −9.26-V sample bias. The energy scale at the bottom is the two-photon intermediate state relative to the bulk Fermi energy plus the saturated surface photovoltage, i.e., the quasi-Fermi level at the surface. The logarithm of electron counts per 5-s interval is plotted.

probe pulses and an assumed exponential lifetime of the intermediate state, as listed in the figure. The excited-state lifetimes obtained in these one-color (4.66-eV) experiments are consistently shorter than those obtained when the pump photon energy was 2.33 eV. Only in intermediate states very close to E_F is there a transient population persisting substantially longer than the pulse width, e.g., the 17-ps lifetime observed at $E_i=0.21$ eV. The data in Fig. 5 are all for intermediate states within the band gap, but the lifetime already approaches the resolution limit with 3-ps pulses in states just 0.46 eV above the valence-band edge.

B. Si(111)7×7

Si(111) wafers doped with boron to 1-Ω cm resistivity were cleaned by the Shiraki method,[42] in which the sample was given a series of wet chemical treatments to remove contaminants and native oxide, finally capping the surface with solution-grown thin oxide for transport to the vacuum system. Annealing at 800 °C in UHV desorbed the oxide cap and left a 7×7 reconstructed surface verified by LEED. Auger analysis performed at the conclusion of each photoelectron experiment showed that the surfaces remained clean, with typical peak ratios of O(KLL)/Si(LMM) <0.005 and C(KLL)/Si(LMM) <0.02.

Figure 6 shows photoelectron spectra obtained under excitation by 3-ps pulses of 4.66-eV light, with intensity varying from 0.12 to 14.5 MW/cm.[2] The sample was biased at −9.26 V. The peak at 9.35 eV was found to be approximately linear in laser intensity. This peak broadens and shifts to higher energy as a function of laser intensity due to the surface photovoltage induced. The width (at 10% points) of the 9.35-eV peak increases from 0.33 to 0.66 eV between the lowest and highest power densities shown. A surface-photovoltage induced broadening or smearing of the type observed may be expected, since the intensity distribution through the laser spot is not a top-hat profile, but is approximately Gaussian. However, the double-peaked structure found on this and all other Si 7×7 samples is not obviously attributable to photovoltage variations within a Gaussian laser spot.

The energy scale E_i shown at the bottom of Fig. 6 requires some comment because of the photovoltage shift. The Fermi level is not well defined in the photoexcited region of the crystal that this experiment probes. The quasi-Fermi level may be considered to vary with depth in the excited crystal due to the transient change in band bending. In Fig. 6, it can be seen that the photovoltage increases as intensity changes from 0.124 to 14.5 MW/cm^2, reaching a value of 0.3 eV based on the shift of the linear photoemission peak. The 9.35-eV peak arises from the surface states that pin E_F. The maximum photovoltage that can occur on 1-Ω cm p-type Si(111)7×7 is the band bending (in darkness) of 0.4 eV. Thus, the bands are approximately flat during the measurement of the highest-intensity spectrum in Fig. 6. Since the two-photon portion of the spectrum comes mainly from the most intense part of the laser spot, it is appropriate to define E_i for the flat-band condition in discussing the two-photon photoemission data.

If we agree to define E_i relative to the quasi-Fermi level at the surface, i.e., the Fermi level in darkness plus the photovoltage shift E_{spv} for the case of flat-band condi-

tions, then Eq. (1) still holds and we may directly compare bulk and surface intermediate states to those on other surfaces, such as $\sqrt{3}\times\sqrt{3}$. Note that in the presence of a photovoltage on a p-type sample, occupied surface states giving one-photon photoemission can be found transiently above the bulk Fermi level, by an energy up to E_{spv}. The band-bending depth on 1-Ω cm silicon is much larger than the photoelectron escape range. Therefore, both bulk and surface features in the laser photoelectron spectrum are shifted rigidly by E_{spv} relative to the bent-band condition obtained in the dark or at low intensity.

The feature at $E_i=0.5$ eV corresponds in energy to the CBM, as studied previously by Long *et al.*[8,10] The entire spectrum in Fig. 6 is very similar to that measured earlier in Ref. 7, despite the much shorter 3-ps pulse duration of the present work. Halas and Bokor[13] reported a very similar spectrum with 60-ps pulses at 4.66 eV on Si(111)2×1. The similarity of spectra obtained with very different pulse widths is, to some degree, surprising, since intermediate states with long lifetimes should contribute less as the laser pulse decreases below the intermediate-state lifetime. In fact, our data show that from the CBM upward, the intermediate-state lifetimes are shorter than or comparable to our 3-ps pulses. We have not yet reached the regime where pulse duration should alter the two-photon region of the spectrum. Bumps in the hot-electron plateau at $E_i=1.84$, 3.3, and 3.98 eV will be discussed later.

Photoelectron counts are plotted against relative delay of 4.66- and 2.33-eV pulses in Fig. 7. The data presentation is as described earlier for Fig. 3, where the electron energies are labeled by the intermediate state E_i. Figure 7 shows that for $E_i=0.12$ eV, the lifetime is about 120 ps, but that it drops sharply at $E_i=0.29$ eV. Recall that

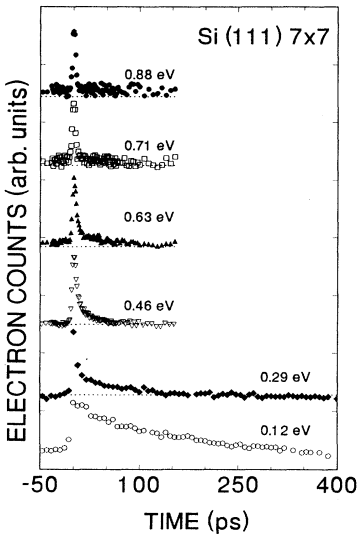

FIG. 7. Time-resolved two-photon photoemission plotted as a function of delay between the 2.33-eV excitation pulse and the 4.66-eV probe pulse. The curves are labeled by the intermediate-state energy relative to the surface quasi-Fermi level. The CBM corresponds approximately to $E_i=0.5$ eV on this scale. Pulse durations were 3 ps.

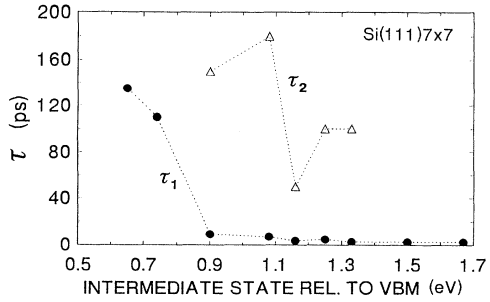

FIG. 8. The intermediate-state lifetimes obtained by fitting the data of Fig. 7 are plotted vs intermediate-state energy measured relative to the valence band edge (VBM). Values of τ_1 were obtained by deconvoluting the laser pulse widths.

E_i on this surface is measured relative to the surface quasi-Fermi level, E_F(dark)$+E_{spv}$. The zero of E_i at the illuminated surface lies within the surface states that pin E_F in the dark.

The data have been fit to two components of exponential decay, as summarized in Fig. 8, where the lifetime components are plotted versus the intermediate-state relative to the valence-band edge in flat-band conditions. The flat-band (nonequilibrium) surface Fermi level is taken to be 0.6 eV above the VBM, corresponding to the states that pin E_F in the dark. It is taken as $E_i=0$ in Figs. 6 and 7, and corresponds to the peak of the linear surface-state photoemission. The data of Fig. 8, for intermediate states referenced to the VBM, show that the principal lifetime τ_1 decreases strongly, from 120 to 10 ps, at about 0.3 eV below the CBM. It decreases again on traversing the conduction-band edge, changing from 7 ps at 0.04 eV below the CBM to 4 ps at 0.04 eV above the CBM, where the CBM energy is 1.12 eV. Intermediate states higher than 0.2 eV above the conduction-band edge exhibit uniformly short lifetimes ≤ 2.5 ps, essentially at the deconvolution limit with 3-ps pulses. There is a second (slow) lifetime plotted in Fig. 8 which is about 150 ps for E_i within the band gap. It decreases suddenly above the conduction-band minimum and simultaneously becomes much weaker.

C. Si(100)2×1

Silicon wafers with (100) surfaces and p-type conductivity (boron, 1 Ω cm) were sputtered and annealed at 1000 °C to produce double-domain 2×1 surface reconstruction,[43,44] which we verified by LEED observations. The photoelectron spectra in Fig. 9 were measured under excitation by 3-ps pulses of 4.66 eV light at intensities from 0.57 to 34.7 MW/cm.^{2} The sample bias was −9.25 V.

The work function of Si(100)2×1 is 4.9 eV.[44] The Fermi level is pinned 0.2±0.2 eV above the valence-band maximum. The small peak at 9.39 eV is linear in laser intensity, in agreement with the location of E_F in Fig. 9. However, the fact that linear (one-photon) photoemission can be excited at all by 4.66-eV light on a surface considered to have a 4.9-eV work function deserves com-

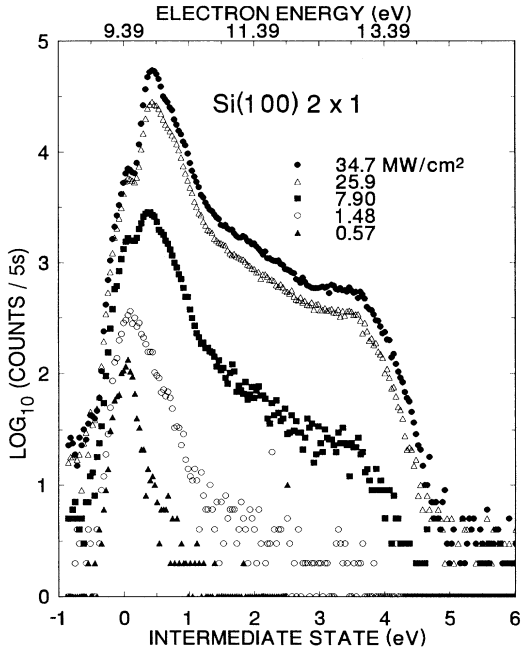

FIG. 9. Photoelectron spectra for Si(100)2×1 excited by 3-ps pulses of 4.66-eV light at the peak intensities shown. The energy scale at the top is the measured electron kinetic energy, including the −9.25-V sample bias. The energy scale at the bottom is the two-photon intermediate state relative to the Fermi energy as zero.

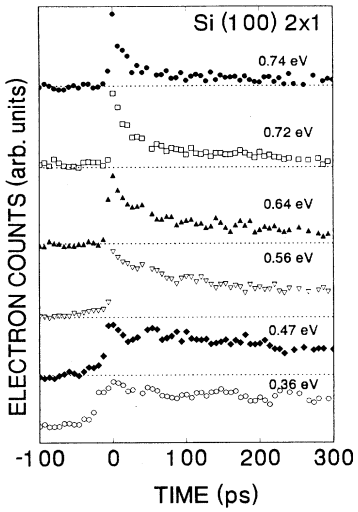

FIG. 10. Time-resolved two-photon photoemission plotted as a function of delay between the 2.33-eV excitation pulse and the 4.66-eV probe pulse. The curves are labeled by the intermediate-state energy relative to the Fermi level. The CBM corresponds approximately to 0.92 eV. Pulse durations were 3 ps.

ment. The one-photon peak at 9.39 eV ($E_i=0$) in Fig. 9 is weak compared to the two-photon spectrum, with a linear photoelectron yield only of order 10^{-8}. As noted above, the Si(100)2×1 surface is double domain with considerable local disorder along the domain boundaries. We suggest that defective areas with nonuniform work functions and associated patch fields are generally responsible for the escape of a few photoelectrons under 4.66-eV illumination. The 9.39-eV peak does not shift with increasing laser intensity, so we conclude that there is no substantial band bending on this surface. This is consistent with the fact that the bulk Fermi level of our 1-Ω cm sample coincides approximately with the surface pinning energy 0.2 eV above the VBM.

The strong peak at $E_i=0.4$ eV and the shoulder and plateau above it are quadratic in laser intensity, arising from two-step excitation via a normally unoccupied intermediate state at 0.4 eV. Its position matches very well the location of the dangling-bond π^* surface state of the dimer model for this surface.[45–47] In Fig. 9, the CBM feature at $E_i=0.92$ eV (relative to E_F) is a weak shoulder, just as it was on the (111) surfaces.

Two-pulse delay curves similar to those discussed in the previous section were measured on the 2×1 surface and are presented in Fig. 10. The excitation pulse is at 2.33 eV and the probe is at 4.66 eV. Lifetimes of the intermediate surface states in the gap are observed to be substantially longer on Si(100)2×1 than on either Si(111)$\sqrt{3}\times\sqrt{3}$-B or Si(111)7×7. Lifetimes on the 2×1 surface are plotted against intermediate-state energy relative to the valence-band edge in Fig. 11. As will be discussed later, the sudden appearance of a short lifetime for $E_i > 0.56$ eV can be attributed to relaxation within the π^* surface-state band and surface recombination near the bottom of the π^* band.

D. Laser-annealed Si(111)1×1

Pulsed laser annealing of Si(111)7×7 induces a surface with a basic 1×1 LEED pattern attributed to disordered short-range 2×1 domains,[48] and/or a mixture of small domains of $c(4\times2)$ and 2×2 reconstruction with no long-range order.[49] In the present work, Si(111)7×7 samples were annealed by 3-ns pulses of 532-nm light in UHV, using two different optical setups for the annealing. In one format using annealing optics that were independent of the photoelectron measurement beam path, a 4-mm-diameter annealing spot was produced with an energy fluence of 0.6 J/cm.[2] The large spot size allowed LEED characterization of the annealed spot, as well as

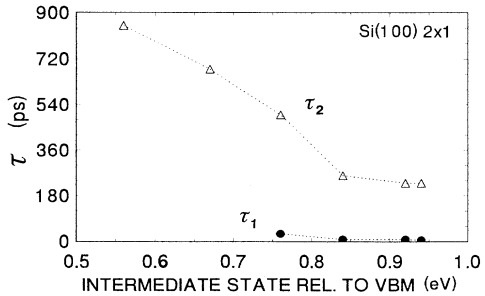

FIG. 11. The intermediate-state lifetimes obtained by fitting the data of Fig. 7 are plotted vs intermediate-state energy measured relative to the valence-band edge (VBM).

accurate determination of the energy fluence. The LEED characterization of silicon samples annealed at 0.6 J/cm^2 per 3-ns pulse showed the expected transition to a 1×1 pattern. However, since the sample had to be moved between the annealing-LEED station and the photoelectron analyzer, the same 10-μm spot was not necessarily measured by photoemission before and after the anneal. Photoelectron spectra measured on the samples annealed at 0.6 J/cm^2 were very similar to the spectra found for the 7×7 surface. This is consistent with the similarity of electronic structures noted in studies of ultraviolet photoemission[50] and in STM spectroscopy.[49]

In order to look for subtle changes in the photoelectron spectrum and in time dependence as a function of annealing, a second optical format was employed, in which the Q-switched annealing pulse was brought in through the same optics used for the photoelectron measurements, and the sample was not moved. This has so far precluded doing LEED on the annealed spot, which was limited to about 0.5-mm diameter. Although the focal plane of the ultraviolet beam used for measurement can be accurately determined as described earlier, the spot area of the annealing pulse was known only within about a factor of 2, with corresponding uncertainty in the energy fluence. In practice, we started at low annealing fluence and increased it while observing changes in the photoemission spectrum or intermediate-state lifetime. This method was used for most of the annealing data, and specifically for the data shown in Figs. 12 and 13.

Figure 12 shows electron-energy spectra measured on the same spot before and after annealing by 20 pulses of energy fluence ≈1.5 J/cm^2 at 532-nm, 3-ns duration. The sample was 1-Ω cm p-type Si(111), and had 7×7

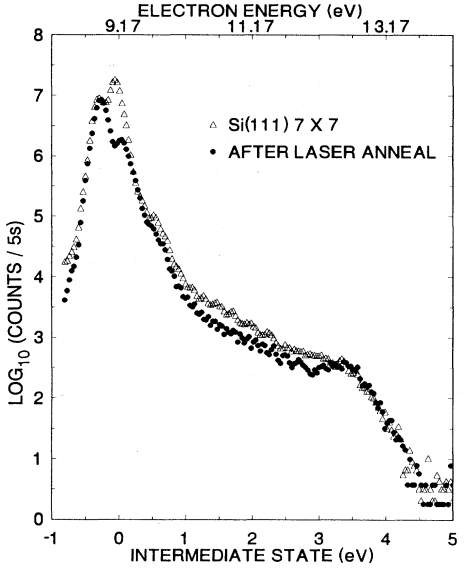

FIG. 12. Photoelectron spectra before and after pulsed-laser annealing of Si(111)7×7 are shown. The pulsed-laser anneal (20 shots at ~1.5 J/cm^2, 532 nm, 3 ns) was confirmed in separate experiments to induce a 1×1 LEED pattern. The photoemission is excited by 3-ps pulses of 4.66-eV light at ~20 MW/cm^2. The energy scale at the top is the measured electron kinetic energy. The energy scale at the bottom is the two-photon intermediate state relative to the surface quasi-Fermi level.

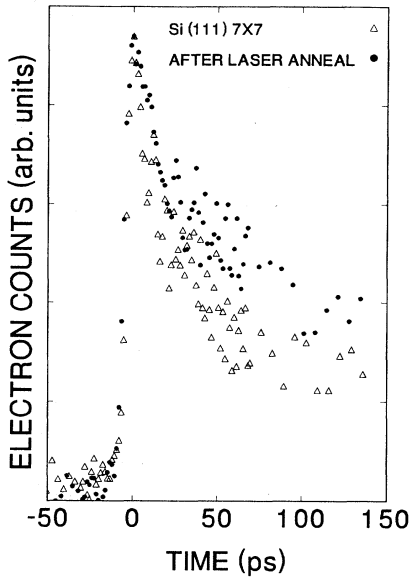

FIG. 13. Time-resolved two-photon photoemission plotted as a function of delay between 3-ps pulses of 2.33-eV excitation and 4.66-eV probe light. The open triangles are for the Si(111)7×7 surface before pulsed-laser annealing. The closed circular points were measured on the same spot after pulsed-laser anneal (20 shots at ~1.5 J/cm^2, 532 nm, 3 ns), which should induce a 1×1 LEED pattern. These measurements were made for electron energy corresponding to intermediate states 0.5 eV above the surface quasi-Fermi level, i.e., near the CBM.

structure before annealing. The most significant change is a sharp reduction in emission from states slightly below E_F', the surface quasi-Fermi level, which is taken as the zero of intermediate-state energies in Fig. 12. The shoulder at about 0.3 eV below E_F remains unchanged. In our earlier discussion of data on the 7×7 surface, the low-energy shoulder was suggested to come from regions of shifted E_F' due to lower intensity and smaller photovoltage shift in the periphery of the Gaussian laser spot. Even in that context, the reason for persistent presence of a resolved shoulder was not clear. The emission from intermediate states above the CBM appears to be slightly depressed after laser annealing, suggesting that the surface has a role in emission associated with hot-electron intermediate states. These trends were reproduced on all three runs made with the second annealing setup. In the experiment conducted with the 4-mm annealing spot, near-threshold fluence of 0.6 mJ/cm^2, and LEED verification of 1×1 reconstruction, the entire spectrum including surface states resembled that of Si 7×7. The noticeable reduction in emission from states near E_F', as observed in Fig. 12, appears to involve modifications continuing beyond the onset of nominal 1×1 reconstruction observed in LEED. Since the 1×1 pattern found for pulsed laser annealing of silicon (111) is not a single-domain structure,[48,49] there are likely to be significant differences in the surface states depending on details of the pulsed annealing procedure. Work is continuing on this question.

Time-resolved measurements are shown in Fig. 13, comparing data on the same spot before and after laser

annealing by 20 pulses of 532-nm, 3-ns light at ≈ 1.5 J/cm.[2] The electron energy selected corresponds to an intermediate state 0.5 eV above the surface quasi-Fermi level, so that the CBM is probed. Comparison of the "before-anneal" data to Fig. 6 shows some sample-to-sample variability in the fractional contribution of the long-lifetime component on our Si 7×7 samples. As discussed later in the general consideration of gap states, the long lifetimes overlapping surface-state bands, as on the 7×7 surface, are almost certainly due to isolated bulk or surface defects. This trend agrees with our assessment of the relative quality of the 7×7 LEED patterns characterizing the samples used for Figs. 6 and 13; i.e., better surface for the data of Fig. 6. This underscores the need to assess effects of annealing on the same spot before and after exposure. Figure 13 shows that both the short and long components of the intermediate-state lifetime at the CBM are increased by pulsed laser annealing under the conditions described.

E. Tunable dye laser pulses on sputtered and annealed Si(111)

In this section, we report experiments conducted on Si(111) prepared by argon ion sputtering and standard 900 °C annealing intended to produce a 7×7 reconstruction. LEED was not performed. Investigations were conducted with frequency-doubled 1.2-ps dye laser pulses tunable from 3.92 to 4.2 eV on these samples. Higher-energy, nontunable photons at 4.66 eV were adopted for most of the later studies reported above. The extra 0.66 eV relative to the 4-eV electron affinity of Si allowed us to probe surface states within the gap, and generally to access one-photon transitions from the vicinity of the Fermi level with 4.66-eV photons. In contrast, photon energies in the 3.92–4.2-eV range lie entirely below the work function of Si(111)7×7, allowing us to study pure two-photon photoelectron emission, at higher intensities obtained by cavity-dumping the synchronously pumped dye laser. Even though intensities up to 580 MW/cm^2 were produced on the sample, the peak temperature rise of the sample remained below 85 °C. Parameters characterizing the experiments with 4-eV light are summarized in Table I.

A photon energy of 4.0 eV corresponds to the electron affinity of Si(111)7×7, so that intermediate states from the CBM up to E_F+4 eV will be probed. Linear photoemission from filled states near E_F should be absent. Figure 14 shows this to be the case, with zero signal at $E_i=0$. Pulses of 4-eV light at 1.2-ps duration and at intensities from 14 up to 584 MW/cm^2 were used. All parts of the spectrum depend quadratically on the laser intensity. Because of the absence of one-photon photoemission, the signal from the region of the transiently populated conduction-band minimum and possible surface states overlapping the CBM can be seen more clearly. The CBM feature which appeared only as a shoulder in Fig. 6 is a substantial peak in Fig. 14. Its low-energy edge (i.e., the actual conduction-band minimum) is suppressed because it is just at the photoemission threshold for 4-eV photons. The main peak extends to intermediate states almost 1 eV above the CBM, followed by a plateau extending up to the topmost populated intermediate state at E_F+4 eV.

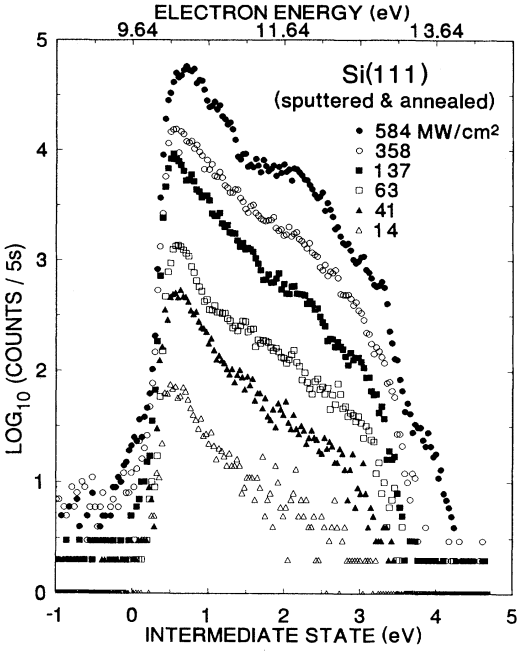

FIG. 14. Photoelectron spectra for sputtered and annealed Si(111) excited by 1.2-ps pulses of 4.0-eV light at the peak intensities shown. The energy scale at the top is the measured electron kinetic energy. The energy scale at the bottom is the two-photon intermediate state relative to the surface quasi-Fermi level plus the saturated surface photovoltage as zero.

Bensoussan *et al.* also measured photoelectron spectra from Si(111)7×7 with 4-eV light, using 5-ns laser pulses.[5] The electron spectra in Ref. 5 are plotted on linear scales and so represent only the upper one or two decades of the spectra shown in Fig. 14. Taking this into account, the parts of their spectra more than 1 eV above the vacuum energy are in reasonable correspondence with our data. Near the vacuum level, however, the energy-distribution curves of Bensoussan *et al.* rise much more slowly than the EDC's of Fig. 14, so that the CBM is completely suppressed. They used a four-grid retarding-field collector with charge amplifier, whereas we have used a double-pass CMA and electron counting detection with the sample biased at ≈ -9.5 V to improve CMA transmission of electrons emitted with energies near the vacuum level. Based partly on correspondence of our $h\nu=4.66$ eV spectra to others measured with CMA (Ref. 8) and time-of-flight[13] analyzers, we are confident that electron emission under 4-eV excitation from states near the conduction-band minimum is correctly represented in Fig. 14.

Figure 15 compares two-photon photoemission spectra measured with variable photon energies from 3.92 eV up to 4.66 eV. The 3.92–4.19-eV light was comprised of 1.2-ps pulses at an intensity of 370 MW/cm^2 on sample. The 4.66-eV light was characterized by a 3-ps pulse duration at 11 MW/cm.[2]

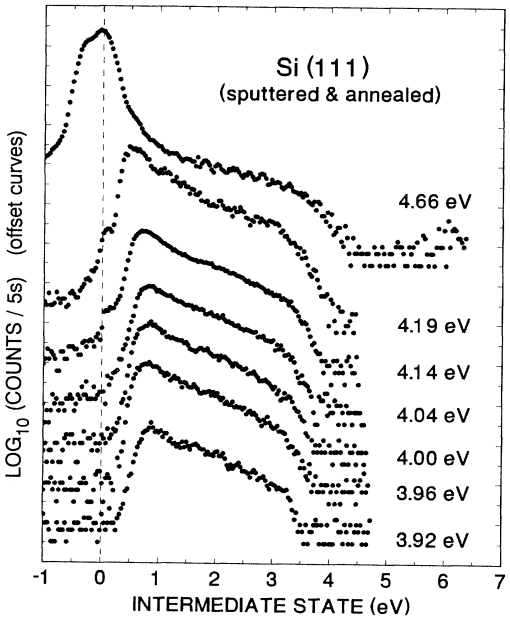

FIG. 15. Two-photon photoemission spectra on sputtered and annealed Si(111) for various photon energies in the range 3.92–4.66 eV. Pulses of 3.92–4.19-eV light were 1.2 ps in duration at a 4-MHz repetition rate and a 370 MW/cm^2 peak intensity. Pulses of 4.66-eV light were 3 ps in duration at 82 MHz and 11 MW/cm^2. The energy scale at the bottom is the two-photon intermediate state relative to the surface quasi-Fermi level. The logarithmic spectra have been offset vertically for convenient display.

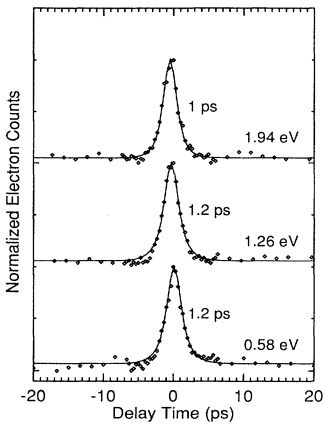

FIG. 16. Time-resolved photoemission plotted as a function of delay between two identical 1.2-ps pulses of 4.0-eV photons on sputtered and annealed Si(111). The data are labeled by the intermediate-state energy relative to the surface quasi-Fermi level. The curves through the data are the result of convoluting the 1.2-ps pulse widths with a single exponential lifetime of the intermediate state, as listed in the figure.

Time resolution of the intermediate-state occupation was measured with 4.0-eV photons in the one-color format discussed previously. Data are shown in Fig. 16 for intermediate states labeled by E_i relative to $E_F+E_{\rm spv}$. The energy $E_i=0.58$ eV corresponds approximately to the conduction-band minimum, so that the data shown are for intermediate states in the conduction band, up to about 1.3 eV above the CBM. The data have been fit by convolution of the 1.2-ps pulses with an assumed exponential decay of the intermediate-state population. The lifetimes determined in this way are all of order 1 ps. These should be regarded for the present as upper limits to the lifetimes, since they are so close to the pulse duration. It is interesting that there is very little increase of the observed lifetime at the CBM, relative to states 1.3 eV higher in energy. An important factor in this will be discussed later in terms of electron diffusion.

Very weak linear photoemission from states near $E_F+E_{\rm spv}$ could be observed from these samples by collecting electrons emitted along the normal to the surface. Such emission should not occur with 4.19-eV light on a single-domain Si(111)7×7 surface, since the work function is 4.6 eV. By changing the sample bias, it was shown that the signal represents photoelectrons emitted from the sample rather than an artifact of reflected light striking some other surface. By turning the sample so that electrons emitted normal to the surface did not enter the CMA, we could exclude this feature from the spectra, or at least minimize it. The spectra of Figs. 14 and 15 were obtained with this sample orientation, but a remnant of the anomalous feature persists in the spectra for $h\nu=4.14$ and 4.19 eV in Fig. 15. After a great deal of worrying with this feature on the early sputtered and annealed samples we have hypothesized, in retrospect, that it was a manifestation of an imperfect reconstruction. Defective regions are presumed to have caused a spatially nonuniform work function.

Note that the average photon fluxes used in these experiments, $\sim 10^{16}$ photons/s, are far in excess of typical uv light sources used in the early studies of silicon photoemission near threshold, and substantially exceed the monochromatic flux of most synchrotron radiation beam lines. The effective photoyield of the anomalous linear photoemission peak was $\approx 10^{-8}$, certainly falling in the category of minority-site emission. Although it is not well characterized or understood, we mention the anomalous peak here as a possible example of minority-site emission occurring below the macroscopic photoelectron threshold. A similar phenomenon was noted in relation to the Si(100)2×1 (double-domain) data in Fig. 9. The transverse components of patch fields that normally draw electrons emitted from a low work-function minority area to the neighboring regions of higher work function cancel along a specific trajectory, e.g., the normal to a flat surface with cylindrical symmetry around the defect site. Since our sample is biased at ≈ -9.5 V, an electron that escapes the surface along such a trajectory will reach the detector with finite kinetic energy. This is consistent with the strongly peaked direction of normal emission and extremely low photoyield that are observed for the anomalous peak.

IV. DISCUSSION

A. Comparison of spectra

Figure 17 compares the two-photon photoelectron spectra for all four surfaces studied. The spectra are plotted against the E_i energy scale of intermediate states defined by Eq. (1), with $E_i=0$ at the Fermi level on samples with no band bending, and $E_i=0$ at $E_F'=E_F(\text{dark})+E_{\text{spv}}$ on samples exhibiting a surface photovoltage saturated at E_{spv}. In the following, we will refer to the reference energy generally as E_F', including the case $E_{\text{spv}}=0$. Figure 17 shows that all four spectra terminate at the maximum intermediate-state energy that can be populated by 4.66-eV photons, given by

$$E_m=E_F'+4.66\text{ eV} . \tag{2}$$

Since these spectra are aligned at the respective E_F', there is no particular alignment of band-structure features in this presentation.

To show correspondences to the band structure explicitly, the same data are presented in Fig. 18, with the spectra aligned to place the valence-band maximum at $E=0$. The VBM was located relative to E_F in each case based on the known doping concentration. Dotted lines indicate the conduction-band minimum at 1.12 eV and a step edge found consistently at 3.9 eV.

B. The conduction-band minimum

Figure 18 shows that a peak or shoulder is always found at the intermediate-state energy corresponding to the conduction-band minimum. Although consistently present, it is in no case a strong feature. This may seem surprising at first in view of anticipated slower relaxation rates of electrons at the CBM compared to hot electrons, and the large sample volume (escape depth) of bulk conduction-band states probed by low-energy photoelectrons compared to the number of surface states. In fact, the spectra presented above are dominated at the low-energy end by surface states. There are two important reasons that the CBM signal is not relatively stronger in these experiments. We shall see below that if conduction electrons were generated instantaneously in the 4.8-nm absorption depth of 4.66-eV light, they would diffuse into the bulk with an initial time constant of about 12 fs. Furthermore, inspection of the silicon band structure shows no final state 4.66-eV directly above the conduction-band minimum. The nearest final state available for a momentum-conserving transition from the conduction band near X is at least 7 eV above the CBM.[51] Therefore, electrons photoemitted from the CBM by 4.66-eV light must have been scattered to final states elsewhere in the Brillouin zone, having a larger velocity projection on $\langle 111\rangle$.

Because surface states are localized spatially in the coordinate normal to the surface, transitions to a continuous spectrum of final states in vacuum with momenta normal to the surface are possible. Thus, surface resonances will dominate the photoemission in this particular photon-energy range, if they are present. The "CBM shoulder" on all four surfaces studied might result from population feeding to a surface resonance from the conduction band at that energy. If that is the case, then our time-resolved measurements have shown rapid (≤ 3 ps)

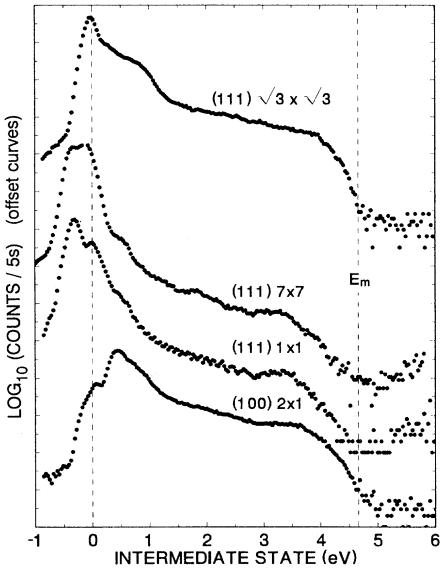

FIG. 17. Two-photon photoemission spectra for four silicon surfaces are plotted against intermediate-state energy referenced to the Fermi energy plus saturated photovoltage. The photon energy is 4.66 eV. The data correspond to the highest intensities in Figs. 1, 6, 9, and 12. The maximum intermediate-state energy that can be populated by the excitation photon is shown as E_m, defined in Eq. (2).

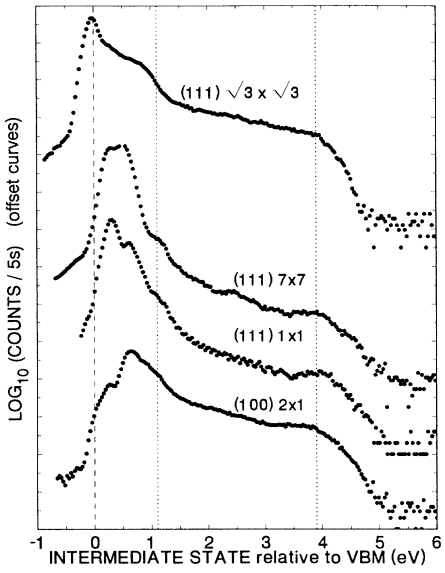

FIG. 18. Two-photon photoemission spectra for four silicon surfaces are plotted against intermediate-state energy referenced to the valence-band edge (VBM) as zero. Also marked by dotted lines are the conduction-band minimum and a consistent peak or step found 3.9 eV above the valence-band edge. The photon energy is 4.66 eV. The data correspond to the highest intensities in Figs. 1, 6, 9, and 12.

equilibration between the CBM and such degenerate surface states. Following the experimental demonstration of rapid equilibration, the photoelectron signal can be regarded as a record of near-surface population in the conduction band even if the emission is attributed to the surface states. Measurements of **k**-resolved inverse photoemission[52] and scanning tunneling spectroscopy[53] have revealed an unoccupied surface state on Si(111)7×7, located 0.5 eV above E_F at $\bar{\Gamma}$. This places it roughly coincident in energy with the conduction-band minimum, so that it is a candidate for the intermediate state we observe at the CBM energy on the 7×7 surface. STM spectroscopy shows that this surface state is uniformly distributed on the 12 adatoms of the 7×7 surface unit cell.[53] The laser-annealed Si(111) surface has been characterized as being very similar in electronic structure to the 7×7 surface, and is therefore a reasonable candidate to have a similar surface resonance degenerate with the CBM. We have already seen that the $\sqrt{3}\times\sqrt{3}$ surface has an occupied surface-state band overlapping the CBM energy. Recall that it was attributed to the dangling-bond orbital on the silicon adatoms in analogy to the 7×7 surface, hence the apparent commonality of this feature. According to the calculation of Chadi,[45] the top of the unoccupied surface-state band in the gap of Si(100)2×1 extends almost to the conduction-band minimum.

An alternative interpretation of the CBM feature can be given in terms of indirect transitions from the bulk conduction band. Evidence for this interpretation comes from hydrogen dosing of the 7×7 surface.[8] Exposure to atomic hydrogen did not alter the results of two-photon photoemission experiments in the CBM region of Si(111)7×7. Also, dosing the Si(111)2×1 surface with O_2 did not diminish the CBM feature, and it was more readily observable with 4.66-eV than with 10.2-eV probe photons.[13]

In the above discussion, we have already answered a puzzle posed earlier concerning CBM emission from (111) and (100) surfaces excited by 4.66-eV light. That is, even if the silicon band structure allowed a 4.66-eV direct transition from the CBM near X, such electrons would lack sufficient $\langle 111\rangle$-projected velocity to escape the (111) surface ($\chi=4$ eV on 7×7), whereas escape from the (100) surface should occur readily. The experimental fact that the conduction-band feature has almost identical strength on (111) and (100) surfaces simply confirms the point already made—there is no X final state 4.66 eV above the conduction-band minimum. All CBM emission observed with our available photon energies is due to indirect transitions or emission from surface states fed from the CBM, whether on the (111) or (100) face.

C. Diffusion of conduction electrons

The optical-absorption coefficient of silicon is very different at 4.66 and at 2.33 eV. The absorption depth, taken as the reciprocal absorption coefficient (α^{-1}), is 4.8 and 830 nm, respectively, for these two photon energies.[54] The concentration gradient of free carriers near the surface is much higher following absorption of 4.66-eV light, and diffusion into the bulk is correspondingly more rapid. Assuming an infinitesimally short pulse, a simple estimate of the time for the average carrier to diffuse a distance equal to the absorption depth may be made. The mean square diffusion range $\langle r^2\rangle$ attained within a time t following a planar impulse at the surface of a semi-infinite material characterized by diffusion coefficient D is

$$\langle r^2\rangle = Dt \ . \tag{3}$$

Substituting α^{-1} for r, as a characteristic diffusion distance needed to significantly dilute the carriers, and taking $D=20$ cm^2/s,[55] one finds $t\approx 12$ fs for 4.66-eV excitation and $t\approx 340$ ps for 2.33-eV excitation of infinitesimal duration.

The more realistic case of finite pulse duration has been discussed in Refs. 4 and 13, for example, based on the carrier-diffusion equation with generation and recombination terms:

$$\frac{\partial n}{\partial t} = D\frac{\partial^2 n}{\partial x^2} + G - R \ , \tag{4}$$

where n is the carrier concentration, D the diffusion coefficient, G the carrier generation rate (cm^{-3} s^{-1}), and R the recombination rate. A Gaussian time profile of the laser pulse was assumed, giving

$$G = \frac{F}{W}\alpha\frac{(1-r)\exp(-\alpha x)\exp(-\beta t^2)}{h\nu} \ , \tag{5}$$

where F is the laser fluence (J/cm^2), W is the pulse width (s), α is the absorption coefficient (cm^{-1}), r is the reflectivity, and $\beta=4\ln 2/W^2$. The Auger recombination term is

$$R=\gamma n^3 \ , \tag{6}$$

where $\gamma=3.8\times10^{-31}$ cm^6/s.[56] The radiative recombination rate in silicon is negligible for the processes of concern here.

Numerical solution of Eq. (4) for our case of 4.66- and 2.33-eV light shows that the initial decay time of excess electron concentration created by 4.66-eV light matches the laser-pulse profile closely. This demonstrates a quite general result, that for generation pulse widths W satisfying

$$W \geq (D\alpha^2)^{-1} \ , \tag{7}$$

the decay time of excess carrier concentration in the near-surface region due to diffusion scales with the pulse duration. That is, carriers diffuse during the generation pulse, reducing the concentration gradient relative to the value predicted from the optical absorption depth.

For 2.33-eV excitation, $(D\alpha^2)^{-1}=340$ ps, Eqs. (4)–(6) predict a decay of carrier concentration significantly slower than our 3-ps pulses, and we should be able to measure competing processes against the slower diffusion-dominated decay. The fastest decay process for intermediate states E_i higher than the conduction-band minimum should be that of cooling toward the CBM. It is not surprising that the corresponding lifetimes shown in Figs. 7 and 8 are comparable to or less than the 3-ps

pulse duration. In addition, however, the major lifetime component at the CBM is in the range of 3–8 ps for all four surfaces studied. Comparing to the solution of Eqs. (4)–(6) for 2.33-eV excitation, it is apparent that carrier diffusion, Auger recombination, and other bulk-relaxation processes cannot give such short lifetimes at the CBM for the parameters of our experiment. The major mechanism remaining is relaxation through surface states and, ultimately, surface recombination. The apparent importance of surface states in the CBM relaxation dynamics is collateral confirmation of our earlier speculation that the CBM is rendered visible to the 4.66-eV photoemission probe photons primarily because of the role of surface resonances coupling to a continuum of final-state momenta normal to the surface. Previous laser photoemission data were analyzed by Long *et al.*[4] and by Halas and Bokor,[13] yielding very high surface recombination velocities on silicon, e.g., $s \approx 10^6$ cm/s on Si(111)7×7 in Ref. 4. Long *et al.* have applied the theory and numerical fitting procedure of Ref. 4 to our data in Fig. 7, finding that $s \approx 10^7$ cm/s is implied, comparable to the thermal-velocity limit of 4×10^6 cm/s.[57]

D. Gap states and lifetimes

Carriers trapped in surface states within the bulk band gap ($E_i < E_{\mathrm{CBM}}$) will, of course, not be subject to diffusion out of the photoelectron escape range. Experimentally, we observed the longest lifetimes for such states. Figures 4, 8, and 11 establish a general trend of longer lifetimes of surface states lower in the gap, in agreement with the expectation of a decreasing number of decay channels as the excited electron state approaches E_F. Except for Si(100)2×1, the longest lifetimes observed were only about 300 ps, and those only for states approaching E_F. In the upper part of the gap, the principal lifetime was 10 ps or less in all samples.

The Si(100)2×1 surface exhibits in Figs. 10 and 11 primarily a long (> 500-ps) lifetime for states up to 0.7 eV above the VBM. Above that energy, a short lifetime of about 8 ps becomes dominant. The 8-ps relaxation component is not found in states less than 0.7 eV above the VBM. It can be reasonably attributed to cooling within the unoccupied (π^*) surface-state band on Si(100)2×1, which extends from 0.6 eV above the VBM to just below the CBM.[45] The lower half of the gap is empty in Chadi's asymmetric dimer surface-band structure. This is reflected in the (100)2×1 spectrum of Fig. 18. If we take the bottom of the π^* surface-state band to be 0.6 eV above the VBM, then from Fig. 11 the lifetime of the π^* surface state is about 700 ps, comparable to the lifetimes observed[11,13] for the π^* surface state on cleaved Si(111)2×1. As shown in the theory and data of Refs. 11 and 13, the decay of the π^* surface state (and the CBM population) is not an exponential function of time, but appears with a fast and a slow component similar to the trace for $E_i = 0.56$ eV in Fig. 10. The fast ~8-ps decay component at higher energy in the gap was not observed with the pulse widths of Refs. 11 and 13, and was not represented in the theory of surface recombination.[13] It is therefore attributed to relaxation within the surface-state band. The long lifetimes at energies below the bottom of the π^* surface-state band may be due to defect states contributing the finite signal found below mid-gap.

It can also be seen in Fig. 18 that our $\sqrt{3}\times\sqrt{3}$ surface unmistakably has a continuous distribution of (normally unoccupied) surface states throughout the gap. The 7×7 surface is well known to have surface states extending throughout the band gap. The surface-state occupation dynamics exhibited for both surfaces in Figs. 3 and 7 are dominated by lifetimes less than 10 ps, consistent with a distribution of surface states that allows carriers entering from the conduction band to scatter progressively down toward the Fermi level without encountering a significant energy gap in the surface states, except perhaps near E_F. This is quite reasonable for the 7×7 surface, but comparison to the surface-band structure on Si(111)$\sqrt{3}\times\sqrt{3}$-B raises the problem discussed earlier, i.e., the absence of surface states expected in the lower part of the bulk-band gap. Basically, our gap-state lifetime data and photoelectron spectra for the $\sqrt{3}\times\sqrt{3}$ surface are consistent with each other, but both are in conflict with the scanning tunneling spectroscopy and surface-band-structure data.[26–28] Although we discussed earlier the reasons for believing that the surface of our boron-implanted and annealed samples is single-domain $\sqrt{3}\times\sqrt{3}$, it must be considered that the observed states in the lower part of the band gap may be defects not intrinsic to the $\sqrt{3}\times\sqrt{3}$ surface.

In summary, our data on the 2×1 surface give a particularly clear separation of gap-state relaxation into few-picosecond relaxation rates occurring within a surface-state band, contrasted to hundred-ps lifetimes at the edge of a wide surface-state gap. Even slower (~ns) lifetimes characterize relaxation within the gaps of intrinsic surface and bulk states. The responsible states must be presumed to be isolated defects. Our data for the 7×7 surface support this same view, since the surface-state bands extend through most of the bulk-band gap.

E. Bulk-band-structure features in the hot-electron spectrum

After the unoccupied surface states in the gap and the CBM, the next most prominent and persistent spectral feature in the two-photon photoelectron spectrum is the peak or step found at 3.9 eV above the valence-band edge, as marked by a dotted line in Fig. 18. Since the energy scale of Fig. 18 is referenced to the valence-band edge, it is natural to ascribe a consistently observed spectral feature to a peak in the intermediate-state density. We thus look to the silicon band structure for a peak in the density of states at 3.9 eV above the VBM. In the density-of-states spectrum for Si as calculated by Wang and Klein,[51] for example, there is a strong peak 3.8 eV above the VBM, corresponding to the rather flat conduction-band dispersion along Λ. It is also significant for the (111) samples that the momentum of Λ states (approaching L) is directed nearly along $\langle 111 \rangle$, and that the band structure shows a final state available about 4.6 eV above the intermediate states along Λ at roughly 75% of the way to L.

A different explanation for a consistent peak in a plot

such as Fig. 18 might come from appeal to the density of initial states rather than intermediate states, coupled with the assumption that two-photon absorption without energy relaxation in the intermediate state is the main contributor to photoemission in the upper plateau. Then structure in the initial state would be preserved as a feature in the final-state spectrum. Since the strongly populated intermediate state is at $E_{\mathrm{VBM}}+3.9$ eV, we should look for a strong peak in the density of states 0.6 eV below the valence-band edge. The first strong peak in the valence density of states is at L, approximately 1.4 eV below the VBM. Thus, the most satisfactory explanation for the 3.9-eV peak in the intermediate-state spectrum remains the first hypothesis, i.e., the 3.8-eV peak in the density of conduction-band states along Λ. We also suggest that the weaker 2.5-eV feature in Fig. 18 arises from intermediate states at the Γ valley of the conduction band.

ACKNOWLEDGMENTS

We wish to thank J. E. Rowe for many helpful discussions and for providing B-implanted silicon samples. We are grateful to Rebecca K. Reed for assistance with experiments and data plotting. Discussions with J. P. Long and M. N. Kabler have been very helpful. This work was supported by NSF Grants Nos. DMR-8901103 and DMR-9206745.

[1]See reviews presented in *Semiconductors Probed by Ultrafast Laser Spectroscopy,* edited by R. R. Alfano (Academic, Orlando, 1984), Vols. I and II.

[2]W. Eberhardt, R. Brickman, and A. Kaldor, Solid State Commun. **42**, 169 (1982).

[3]H. M. van Driel, J. S. Preston, and M. I. Gallant, Appl. Phys. Lett. **40**, 385 (1982); J. F. Young and H. M. van Driel, Phys. Rev. B **26**, 2147 (1982).

[4]J. P. Long, H. R. Sadeghi, J. C. Rife, and M. N. Kabler, Phys. Rev. Lett. **64**, 1158 (1990).

[5]M. Bensoussan, J. M. Moison, B. Stoesz, and C. Sebenne, Phys. Rev. B **23**, 992 (1981).

[6]M. Bensoussan and J. M. Moison, Phys. Rev. B **27**, 5192 (1983).

[7]J. M. Moison and M. Bensoussan, Solid State Commun. **39**, 1213 (1981).

[8]J. P. Long, R. T. Williams, J. C. Rife, and M. N. Kabler, in *Energy Beam-Solid Interactions and Transient Thermal Processing,* edited by D. K. Biegelsen, G. A. Rozgonyi, and C. V. Shank, MRS Symposia Proceedings No. 35 (Materials Research Society, Pittsburgh, 1984), p. 81.

[9]Lee A. DuBridge, Phys. Rev. **43**, 727 (1933).

[10]J. P. Long, M. N. Kabler, J. C. Rife, and R. T. Williams, in *18th International Conference on the Physics of Semiconductors,* edited by O. Engstrom (World Scientific, Singapore, 1987), p. 1469.

[11]J. Bokor, R. Storz, R. R. Freeman, and P. H. Bucksbaum, Phys. Rev. Lett. **57**, 881 (1986).

[12]J. Bokor, R. Haight, R. H. Storz, J. Stark, R. R. Freeman, and P. H. Bucksbaum (unpublished).

[13]N. J. Halas and J. Bokor, Phys. Rev. Lett. **62**, 1679 (1989); J. Bokor and N. J. Halas, IEEE J. Quantum Electron. **QE-25**, 2550 (1989).

[14]R. T. Williams, J. C. Rife, T. R. Royt, and M. N. Kabler, J. Vac. Sci. Technol. **19**, 367 (1981).

[15]R. T. Williams, T. R. Royt, J. C. Rife, J. P. Long, and M. N. Kabler, J. Vac. Sci. Technol. **21**, 509 (1982).

[16]R. Haight and J. A. Silberman, Phys. Rev. Lett. **62**, 815 (1989); J. Vac. Sci. Technol. B **7**, 910 (1989); IEEE J. Quantum Electron. **QE-25**, 2556 (1989).

[17]R. Haight and J. Bokor, Phys. Rev. Lett. **56**, 2846 (1986).

[18]R. T. Williams, J. P. Long, and M. N. Kabler, Opt. Eng. **28**, 1085 (1989).

[19]J. P. Long, S. S. Goldenberg, and M. N. Kabler, Phys. Rev. Lett. **68**, 1014 (1992).

[20]J. G. Fujimoto, J. M. Liu, E. P. Ippen, and N. Bloembergen, Phys. Rev. Lett. **53**, 1837 (1984); D. Straub and F. G. Himpsel, Phys. Rev. B **33**, 2256 (1986).

[21]K. Giesen, F. Hage, F. J. Himpsel, H. J. Riess, and W. Steinmann, Phys. Rev. Lett. **55**, 300 (1985); D. Rieger, T. Wegehaupt, and W. Steinmann, Phys. Rev. Lett. **58**, 1135 (1987).

[22]S. Schuppler, N. Fischer, W. Steinmann, R. Schneider, and E. Bertel, Phys. Rev. B **42**, 9403 (1990).

[23]G. D. Kubiak, J. Vac. Sci. Technol. A **5**, 731 (1987); Surf. Sci. **201**, L475 (1988).

[24]J. M. Nicholls, B. Reihl, and J. E. Northrup, Phys. Rev. B **35**, 4137 (1987).

[25]A. B. McLean, L. J. Terminello, and F. J. Himpsel, Phys. Rev. B **41**, 7694 (1990).

[26]P. Bedrossian, R. D. Meade, K. Mortensen, D. M. Chen, J. A. Golovchenko, and D. Vanderbilt, Phys. Rev. Lett. **63**, 1257 (1989).

[27]I. W. Lyo, E. Kaxiras, and Ph. Avouris, Phys. Rev. Lett. **63**, 1261 (1989).

[28]E. Kaxiras, K. C. Pandey, F. J. Himpsel, and R. Tromp, Phys. Rev. B **41**, 1262 (1990).

[29]R. L. Headrick, I. K. Robinson, E. Vlieg, and L. C. Feldman, Phys. Rev. Lett. **63**, 1253 (1989).

[30]Y. Ma, J. E. Rowe, E. E. Chaban, C. T. Chen, R. L. Headrick, G. M. Meigs, S. Modesti, and F. Sette, Phys. Rev. Lett. **65**, 2173 (1990).

[31]J. E. Demuth, B. N. J. Persson, and A. J. Schell-Sorokin, Phys. Rev. Lett. **51**, 2214 (1983).

[32]F. J. Himpsel, G. Hollinger, and R. A. Pollak, Phys. Rev. B **28**, 7014 (1983).

[33]F. J. Himpsel, D. E. Eastman, P. Heimann, and B. Reihl, Phys. Rev. B **24**, 1120 (1981).

[34]J. E. Demuth, W. J. Thompson, N. J. DiNardo, and R. Imbihi, Phys. Rev. Lett. **56**, 1408 (1986).

[35]Hanli Liu, M.S. thesis, Wake Forest University, 1990.

[36]D. Burgess, P. C. Stair, and E. Weitz, J. Vac. Sci. Technol. A **4**, 1363 (1986).

[37]J. P. Long, R. T. Williams, T. R. Royt, J. C. Rife, and M. N. Kabler, in *Laser-Solid Interactions and Thermal Processing of Materials,* edited by J. Narayan, W. L. Brown, and R. A. Lemons, MRS Symposia Proceedings No. 13 (Elsevier, New York, 1983), p. 89.

[38]J. E. Rowe, G. K. Wertheim, and D. M. Riffe, J. Vac. Sci. Technol. A **9**, 1022 (1991).

[39]P. Bedrosian, K. Mortensen, D. M. Chen, and J. A. Golovchenko, Phys. Rev. B **41**, 7545 (1990).

[40]I. W. Lyo, E. Kaxiras, and Ph. Avouris, Phys. Rev. Lett. **63**, 1261 (1989).
[41]G. P. Kochanski (private communication).
[42]A. Ishizaka and Y. Shiraki, J. Electrochem. Soc. **133**, 666 (1986).
[43]J. E. Rowe and H. Ibach, Phys. Rev. Lett. **32**, 421 (1974).
[44]M. J. Cardillo and G. E. Becker, Phys. Rev. B **21**, 1497 (1980).
[45]D. J. Chadi, Phys. Rev. Lett. **43**, 43 (1979).
[46]J. A. Appelbaum, G. A. Baraff, and D. R. Hamann, Phys. Rev. Lett. **35**, 729 (1975).
[47]R. J. Hamers, R. M. Tromp, and J. E. Demuth, Surf. Sci. **181**, 346 (1987).
[48]Y. J. Chabal, J. E. Rowe, and D. A. Zwemer, Phys. Rev. Lett. **46**, 600 (1981).
[49]R. S. Becker, J. A. Golovchenko, G. S. Higashi, and B. S. Swartzentruber, Phys. Rev. Lett. **57**, 1020 (1986).
[50]D. M. Zener, C. W. White, P. Heimann, B. Reihl, F. J. Himpsel, and D. E. Eastman, Phys. Rev. B **24**, 4875 (1981).
[51]C. S. Wang and B. M. Klein, Phys. Rev. B **24**, 3393 (1981).
[52]J. M. Nicholls and B. Reihl, Phys. Rev. B **36**, 8071 (1987).
[53]R. J. Hamers, R. M. Tromp, and J. E. Demuth, Phys. Rev. Lett. **56**, 1972 (1986).
[54]D. E. Aspnes and A. A. Studna, Phys. Rev. B **27**, 985 (1983).
[55]J. C. Herper, I. Palocz, N. N. Axelrod, and R. A. Stern, J. Appl. Phys. **45**, 224 (1974).
[56]M. H. Van Driel, Phys. Rev. B **35**, 8166 (1987).
[57]J. P. Long (private communication).